

## RESEARCH ARTICLE



# Practical Sensor Performance and Methodology for Measuring Permittivity of Dielectric Plates in the Microwave Frequency Range

Yuri Choni<sup>1,\*</sup>, Vladimir Lavrushev<sup>1</sup> and Alexander Avksentev<sup>1</sup>

<sup>1</sup>Department of Radio Telecommunication Systems, Kazan National Research Technical University, Russia

**Abstract:** A wide range of microwave devices, particularly those intended for use in telecommunication systems, are manufactured using printed circuit board technology. Designing such devices requires precise knowledge of the properties of the dielectric plates used. In this article, the authors propose a very easy-to-manufacture measuring device that combines the nondestructive testing inherent in the free space method with the ability to achieve the accuracy of the resonance method. Two factors provide the advantages of the proposed installation: the peculiarities of the plates' geometric structure and software processing of the measurement results. One- and two-port designs are considered, and the features of the corresponding algorithms for processing measurement data are investigated. The results of electrodynamic modeling of strip-line fixtures in the CST Studio Suite environment confirm their operability and the possibility of providing sufficiently high sensitivity when measuring the complex permittivity of plates made of various materials. Areas for future research are discussed.

**Keywords:** printed microwave circuit, dielectric plate, complex permittivity, measuring, installation, sensitivity

## 1. Introduction

Depending on the area of application and purpose of the devices in which a particular material is used, parameters reflecting its functional qualities are of great importance. For dielectrics included in the design of various devices, these are the permittivity  $\epsilon = \epsilon' \epsilon_0$  [F/m] and electrical conductivity  $g$  [S/m], characterizing interaction with the electromagnetic (EM) field. Taking into account the field frequency  $\omega$ , they introduce a more significant and convenient characteristic, called the relative complex permittivity of the dielectric:

$$\epsilon' = \epsilon' - jg/\omega\epsilon_0 \quad (1)$$

The ratio of the imaginary part of the quantity  $\epsilon$  to its real part characterizes the attenuation of the EM field in a dielectric and is called the dielectric loss tangent, commonly denoted as  $\text{tg}\delta$ .

Dielectrics have a wide variety of uses. Microwave circuits in general and microstrip circuits in particular are printed on dielectric substrates whose complex permittivity must satisfy strict requirements, especially in terms of small values of  $\text{tg}\delta \approx 0$ . Composite materials for stealth aircraft and materials for coating the walls of anechoic measurement chambers are unique in terms of the role of losses. Here, the requirements for  $\text{tg}\delta$  values are opposite.

In light of the above, it is obvious that, despite the variety of known methods for measuring the parameters of dielectrics and corresponding installations [1–15], their improvement continues to this day [16–32].

This article refers to similar works. Its subject is a very practical, portable, and robust measuring setup [29] for nondestructive measurement of the complex permittivity of dielectric plates.

The results of modeling in the CST Studio Suite software package of several versions of the proposed device, in combination with suitable algorithms for processing measurement data, are presented.

## 2. Literature Review

Even without being an expert in the history of measuring systems' development, one can guess that the very first method of monitoring the parameters of dielectrics was measuring the capacitance of a plane capacitor with the test material between its plates. This simple and reliable method, mentioned in long-standing works [1], is still being improved in various aspects [2–6] and is used primarily in monitoring the parameters of materials for low-frequency installations of power plants and networks [7]. The corresponding setups are present among the measuring equipment produced by such well-known companies as the Chinese "Advanced Power Technologies," the Russian "Micran JSC," and the American "Agilent Technology."

When monitoring the characteristics of materials in the high-frequency range, other methods are more effective. Thus, a new (at those old times) measurement method [1] involves the analysis of the field distribution along a waveguide or coaxial cable with a

\*Corresponding author: Yuri Choni, Department of Radio Telecommunication Systems, Kazan National Research Technical University, Russia. Email: [yuichoni@kai.ru](mailto:yuichoni@kai.ru)

sample of the material inserted at the short-circuited end of it. By the way, a cavity resonator has long been [8] and still is [9, 10] a measuring device that is capable of accurately measuring  $\epsilon'$  by the shift in the resonant frequency and the  $\tan\delta$  by the change in the Q factor of the resonator with an inserted sample.

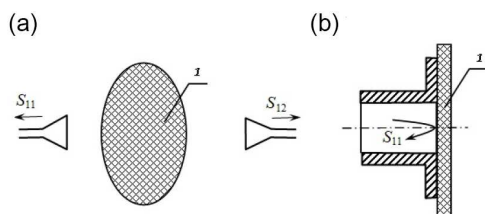
Modern technologies use automated instruments to measure the reflectivity and/or transmittance of a device containing a material sample, making measurements over a range of frequencies rather than at a fixed frequency [10]. Even within the framework of known methods, the arsenal of corresponding sensor modules and data processing algorithms is constantly growing. Examples of this include special-section or dielectric waveguides [11–14], split-cavity resonators [15, 16], innovative installations, and measurement methods [17–19].

### 3. Nondestructive Measurement Technique

#### 3.1. Introductory remarks

Obviously, nondestructive measuring is of great practical interest. The corresponding technology grows out of two methods shown in Figure 1. These are measurements in free space [20–22] when an EM field of a certain frequency irradiates the body under test. Second, the measurement of the reflection coefficient in a waveguide, to the flange of which the measured body is pressed (see page 6, Figure 1d in the review [23]).

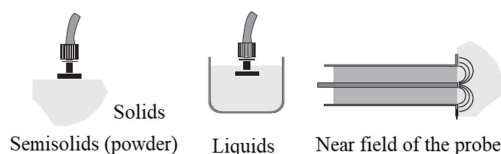
**Figure 1**  
Nondestructive measurements. (a) Free space measurement.  
(b) Waveguard probe



The capabilities of both methods increase significantly with using modern vector network analyzers to record data in digital format and process it in high-performance 3D EM analysis software packages such as CST Studio Suite or another [24, 25, 26]. Unfortunately, both of these methods do not have the necessary sensitivity to measure  $\tan\delta$ .

We would like to warn interested readers against misjudging the merits of the Keysight coaxial probe, shown in Figure 2. In fact, this probe only works for lossy materials. In [6], there is only a hint: “preferably for lossy,” but there are no clearly defined restrictions.

**Figure 2**  
Keysight coaxial probe



The bitter truth is that the coaxial does not radiate through its outer cut into the pressed body and interacts with it slightly through

the near field, which exists in a very small region. Therefore, in the absence of losses, the reflectivity  $S_{11}$  is practically equal to one. Calculations show that in the case of a coaxial cable with a diameter of 2 mm, the value of  $S_{11}$  at a frequency of 1 GHz differs from one only in the sixth decimal place ( $S_{11} > 0.99999$ ) for any dielectric body pressed.

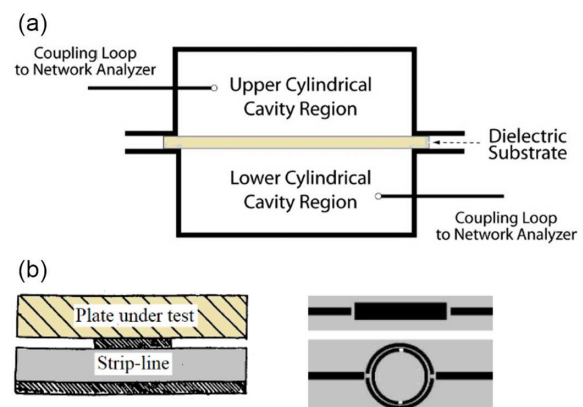
Dielectric plates are widely used in the construction of various microwave devices, especially when it comes to strip or microstrip substrates. That is why methods and means for measuring their complex permittivity are constantly improving.

#### 3.2. Prototypes of the proposed structure

Most often, ideas come to mind out of nowhere, and the search for prototypes does not precede the invention but is carried out after, when submitting its application. In the article, issues close to the topic under discussion should be considered before. It is worth mentioning two solutions for nondestructive measuring the permittivity of dielectric plates.

First, a cylindrical cavity resonator for the  $TE_{011}$  resonant mode [27], which is separated into two halves, as depicted in Figure 3(a). A planar dielectric substrate under test is inserted into the resonator through the gap between its two sections. The merits and disadvantages inherent in any implementation of the resonator method are high accuracy and a sharply limited frequency range of measurements, respectively.

**Figure 3**  
Schemes of measurement fixtures. (a) Split-cylindrical resonator. (b) Strip-line fixture: cross-section (left), two types of resonators (right)



Second, the strip-line fixture shown in Figure 3(b). Its configuration is ideally compatible with the geometry of the dielectric plate under test [28]. In addition, the strips, depending on the nature of the plate material, can differ and form resonators of different types, as shown in Figure 3(b). The disadvantage is the decrease in sensitivity because the test plate is located above the strip where the EM field is weak.

#### 3.3. The proposed strip-line fixture

Our idea is simple: use a strip line that has no dielectric slab, as shown in Figure 4, and insert the measured plate in the gap between the strip and the ground plane [29]. The achievable measurement accuracy corresponds to the measurement methods in feeders or resonators, since the strip may contain resonating fragments.

Figure 4

Appearance of strip-line fixture. (a) Metallic strip. (b) Patch strip

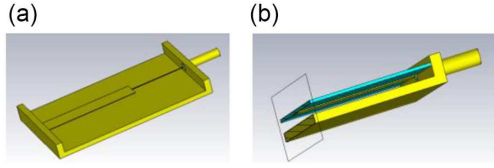
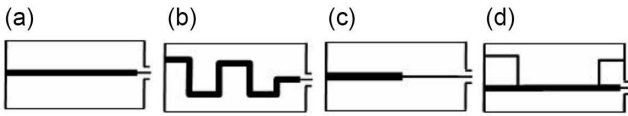


Figure 5 shows some possible strip configurations in the simplest case of measuring the reflection coefficient of a shorted strip line. For a lossy plate, say, made of a radio-absorbing material, the stripe can be uniform and straight (a). Since the sensitivity to the measured parameters increases with the lengthening of the stripe, a meander-like configuration (b) is useful in this regard. Figure 5 (a) and (b) show a line with elements resonating due to an impedance jump or shorted stubs, respectively.

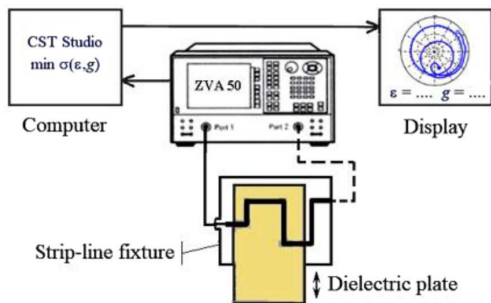
Figure 5

Short-circuited strip-line options. (a) Straight line. (b) Meander line. (c) Non-uniform line. (d) Line with two shunts



Naturally, it is not easy to ensure sufficient strip rigidity in the design of Figure 3(a). If the strip line is printed on the bottom plane of a thin substrate, as shown in Figure 3(b), then not only does the problem of the required rigidity disappear, but it also becomes possible to make splits in the strip to form resonators, such as in Figure 2(b), for example.

Figure 6 shows the block structure and composition of the measuring setup. The dotted line corresponds to the measurement of not only the reflection coefficient but also the transmission coefficient.

Figure 6  
Measuring setup

From a vector network analyzer (ZVA 50 or other), the frequency dependences of the reflection coefficient  $S_{11}(f)$ , and possibly also the transmission coefficient  $S_{21}(f)$ , are loaded into the computer, where a package (CST Studio Suite or other) for the electrodynamic modeling of suitable microwave devices is installed.

### 3.4. Measurement methodology

In general, the process of measuring the relative complex permittivity (1) involves simulating a strip-line fixture with the test plate inserted as it is, while varying the plate parameters  $\epsilon'$  and  $g$ . The  $\epsilon'$  and  $g$  values corresponding to the minimum deviation of the frequency dependences obtained during the simulation from the measured dependences serve as the measurement result.

The advantage of the method under consideration is that it is also operational in cases where the thickness of the dielectric plate is less than the distance between the strip and the ground plane, as well as with an arbitrary plate configuration within the dimensions of the fixture. Due to the design features of the fixture, it is possible to shift the test plate and thereby provide additional control over its homogeneity in the longitudinal direction. The double-headed arrow in Figure 5 hints at this.

Let  $S_{11}(\omega, \epsilon', g)$  be the frequency dependence obtained as a result of modeling for certain values of parameters  $\epsilon$  and  $g$ . A quantitative assessment of the distinction between modeled and measured dependences can be the  $L_2$  norm of the difference between two functions  $S_{11}(\omega)$  and  $S_{11}(\omega, \epsilon', g)$ , which has the meaning of the mean square error. Using conventional notation for the square of the norm of the function  $\|f(\omega)\|^2 = \int_{\omega_{\min}}^{\omega_{\max}} |f(\omega)|^2 d\omega$ , and emphasizing the dependency on the values of  $\epsilon'$  and  $g$ , we have the relative value  $\sigma_1(\epsilon', g)$  of the standard deviation as:

$$\sigma_1(\epsilon', g) = \|S_{11}(\omega) - S_{11}(\omega, \epsilon', g)\|^2 / \|S_{11}(\omega)\|^2 \quad (2)$$

Above,  $\omega_{\min}$  and  $\omega_{\max}$  define the operating range around the nominal frequency  $\omega_0$ .

In cases, when the transmission coefficients  $S_{21}(\omega)$  and  $S_{21}(\omega, \epsilon', g)$  are measured and modeled, their standard deviation  $\sigma_2(\epsilon', g)$  appears similar to the previous one:

$$\sigma_2(\epsilon', g) = \|S_{21}(\omega) - S_{21}(\omega, \epsilon', g)\|^2 / \|S_{21}(\omega)\|^2 \quad (3)$$

The measurement process consists of minimizing the objective function, which in general is the sum

$$\sigma(\epsilon', g) = \sigma_2(\epsilon', g) + \mu \sigma_1(\epsilon', g), \quad (4)$$

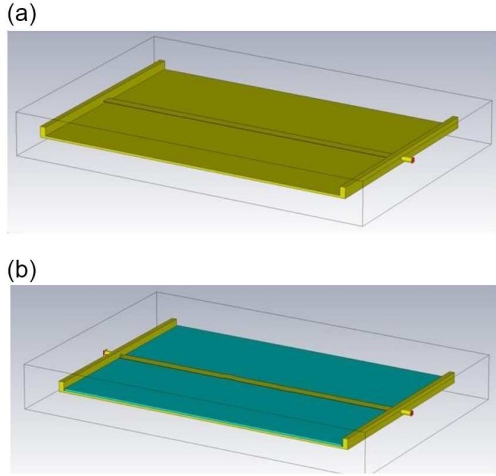
where the weight factor  $\mu$ , being greater or less than one, gives preference to the term that has increased sensitivity to changes in the properties of the material under test.

Since the objective function (4) is not analytic, there is no other way to minimize it except by using time-consuming search algorithms such as global minimizers or coordinate descent methods. If measurements are carried out to clarify the properties of a plate with approximately known values  $\epsilon'_0$  and  $g_0$ , the operator can minimize the function  $\sigma(\epsilon', g)$  manually, observing its current values  $\sigma$  and varying the variables  $\epsilon'$  and  $g$  around their nominal values  $\epsilon'_0$  and  $g_0$ .

Finally, note that during the calibration stage of measurements, the input and output of the fixture are physically set by using a calibration kit. In the simulation, the corresponding ports play the same role. It is not easy to ensure the complete identity of the measurement and simulation results in this respect, since there is some amount of uncertainty in the electrical length of both the coaxial strip connector and the element of the calibration set. For this reason, it is useful to perform preliminary measurements with an empty fixture (without a test plate) and, by varying the port positions during the simulation, achieve coincidence with the measured results. The resulting port settings should be used in all subsequent measurements with this fixture.

Figure 7

Simulated strip-line fixture. (a) Short-circuited line segment. (b) Two-port fixture with inserted dielectric plate



#### 4. Simulation Results

To illustrate the process of measuring the complex permittivity of a dielectric plate using the device under consideration, two strip-line fixtures of the simplest design, made of bronze, were simulated (see Figure 7).

One of them (Figure 7a) is a straight short-circuited strip 0.12 mm thick, 10 mm wide, and 200 mm long, located 2 mm above the ground plane. The transverse dimension of the device was 290 mm, although this does not matter. The input of the fixture was a 50-ohm coaxial port. A dielectric plate of  $200 \times 290 \times 2 \text{ mm}^3$ , located between the ground plane and the strip, played the role of the thing under test.

##### 4.1. Lossy plate under test

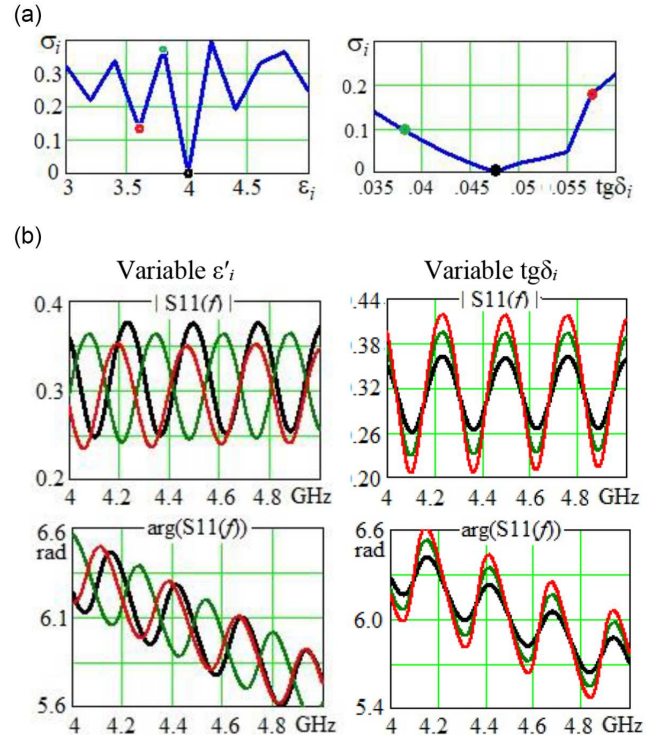
The nominal values of the plate properties were  $\epsilon' = 4$  and  $\text{tg}\delta = 0.047$ . Thus, we are dealing with a lossy material. Figure 8 shows the simulation results for measuring relative permittivity  $\epsilon'$  at a given value of  $\text{tg}\delta = 0.047$  (left column) and  $\text{tg}\delta$  at a given value of  $\epsilon' = 4$  (right column). In Figure 8(a), the black, green, and red bold dots on the graphs indicate three values of  $\epsilon'$  and  $\text{tg}\delta$ , respectively, which correspond to the frequency dependences of the reflection coefficient shown below in the same color.

The variables  $\epsilon'$  and  $\text{tg}\delta$  took discrete values (the index  $i$  emphasizes this) with relatively rough steps of 0.2 and 0.05, respectively, to cover sufficiently wide intervals. Naturally, here and further in the calculations, we used the conductivity  $g$ , determined by  $\text{tg}\delta$ , and the nominal frequency  $\omega_0$  by the equality  $g = \text{tg}\delta \omega_0 \epsilon' \epsilon_0$ . It turned out unexpectedly that the objective function  $\sigma_1(\epsilon')$  has local minima in addition to the global one. Of course, this slightly complicates the process of minimizing the objective function, but the presence of a zero global minimum makes it easy to overcome this difficulty.

To clarify the physical causes that engender the multi-extremal behavior of the function  $\sigma_1(\epsilon')$ , the left column in Figure 8(b) reproduces the frequency dependences of  $S_{11}(f)$ . It is clear that significant losses cause high conductivity in the impedance of the fixture input and, accordingly, small changes in the phase of the reflection coefficient ( $\pm 30^\circ$ ). Depending on the frequency, the phase of the secondary wave reflected from the short-circuited end of the rather

Figure 8

Measuring complex permittivity  $\epsilon$ . (a) Objective function  $\sigma_1(\epsilon')$  and  $\sigma_1(\text{tg}\delta)$ . (b) Reflection coefficient  $S_{11}(f)$



long strip quickly changes from antiphase (for the green curve) to almost in-phase (for the red curve). Therefore, at the corresponding values  $\epsilon'$ , the difference between the current and nominal functions  $S_{11}(f)$  increases or decreases, causing local extrema of the objective function  $\sigma_1(\epsilon')$ .

In addition to algorithmic methods for finding the global minimum, there are also other possibilities. When the measuring line is shortened, local minima move away from the global one, although this also reduces the sensitivity to changes in permittivity. Therefore, if the plate is made of an unknown material, its permittivity can be roughly estimated on one setup, and then the measurement results can be refined on another. In fact, this is a repetition of the classical approach widely used in phase interferometry direction finding systems.

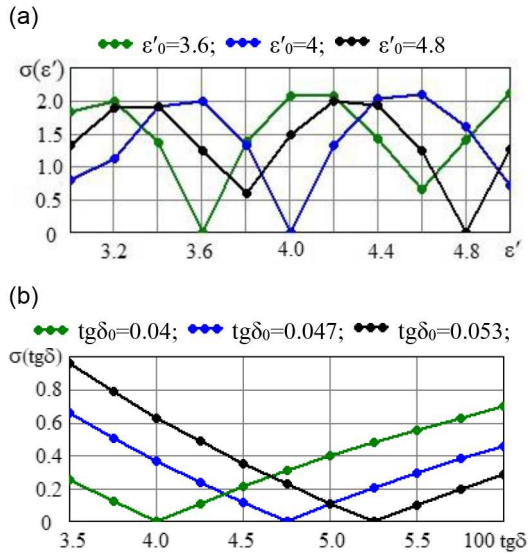
In the right column of Figure 8, similar to the left column, the results of minimization of the objective function  $\sigma_1(\epsilon', g)$  are presented for the nominal value  $\epsilon' = 4$  and variable  $\text{tg}\delta$ . In the calculations, naturally, the conductivity  $g$  is used, the value of which is uniquely related to the values of  $\text{tg}\delta$ , as shown above.

We can see that the function  $\sigma_1(\text{tg}\delta)$  has the only minimum. This is because the change in losses obviously does not affect the phase velocity. Therefore, at each frequency, the phase shift of the secondary wave relative to the initial wave does not change, and the structure of the frequency functions  $S_{11}(\omega, \text{tg}\delta)$  shown below does not change depending on the value of  $\text{tg}\delta$ . This is because the change in losses has virtually no effect on the phase velocity. Therefore, at each frequency, the phase shift of the secondary wave relative to the initial one does not change, and the values of the maxima and minima change but do not shift.

As expected, the calculations confirm that the use of even the simplest two-port fixture, shown in Figure 7b, provides a significant increase in its sensitivity due to handling larger amounts of



**Figure 9**  
Measuring with two-port fixture. (a) Objective function  $\sigma(\varepsilon')|_{\text{tg}\delta=0.047}$ . (b) Objective function  $\sigma(\text{tg}\delta)|_{\varepsilon'=4}$



information. To illustrate the corresponding regularities, the process of measuring the complex permittivity based on the frequency dependences of the reflection and transmission coefficients was simulated. The objective function  $\sigma(\varepsilon', g)$  corresponded to formula (4) with  $\mu = 1$ .

The results for three tested dielectric plates (DPT) with a height of 2 mm,  $\text{tg}\delta = 0.047$ , and nominal permittivity  $\varepsilon'_0$  equal to 3.6, 4, and 4.8 are shown in Figure 9a.

First, the global minima of the functions  $\sigma(\varepsilon')$  exactly correspond to the nominal values  $\varepsilon'_0$ , and their slopes are 3 times steeper than those of the similar curve in Figure 8a on the left for the above case of a short-circuited strip line. This confirms a significant increase in the sensitivity of the measuring setup. Secondly, the existence of local minima is due to the obvious fact that with a certain change in  $\varepsilon'$ , the phase shift of not only the reflected but also the transmitted wave acquires a shift of  $2\pi$ .

Figure 9b illustrates the process of measuring the dielectric loss tangent for three plates with the same permittivity  $\varepsilon' = 4$  and nominal values of  $\text{tg}\delta_0$  equal to 0.04, 0.047, and 0.053, respectively. Please note: to keep the axis labels short, we plot not  $\text{tg}\delta$ , but  $100 \text{tg}\delta$  on the abscissa axis. Comparing the steepness of the objective function  $\sigma(\text{tg}\delta)$  at the global minimum  $\text{tg}\delta = 4$  with that in the previous case (Figure 8a on the right), it is easy to see that the steepness has increased by 4.6 times, and the sensitivity of the measuring setup has improved accordingly.

Hereinafter, dots on the dependence lines denote the set of calculated values.

#### 4.2. Good dielectric under test

The permittivity  $\varepsilon'$  directly affects the phase velocity of the propagating EM field, which clearly affects the reflection and transmission coefficients of any microwave device. Accordingly,  $\varepsilon'$  can be easily measured in a stripe device of various configurations. In contrast, measuring the low-loss tangent inherent in a good dielectric is a serious problem. The resonator method is the only way to overcome it.

Calculations, the results of which are discussed below, give evidence that a strip resonator of the simplest design is acceptable

for the purpose under consideration. For instance, a low-impedance half-wavelength open-circuit stub results in rather intense reflections outside a narrow range around the resonant frequency. The decisive role here is played by the fact that the depth of the dip at the resonant frequency depends significantly on the loss tangent.

Measurements with three dielectric plates, each 2 mm thick and having the same permittivity  $\varepsilon'_0 = 2.1$ , were the subject of the simulation. The plates differed in the loss tangent  $\text{tg}\delta_0$ , the values of which were 0.0014, 0.0017, and 0.0021, respectively.

The measurement fixture consisted of a 6.57-mm-wide strip located 2 mm above the ground plane and forming a 50-ohm feed line between two 50-ohm ports, and a 10-mm-wide open-circuit stub (15-ohm characteristic impedance) in the middle of the line. The stub length was 80 mm, which corresponded to a three-quarter-wave resonance at a frequency of 2.172 GHz. The minimized objective function  $\sigma(\varepsilon', g)$  coincided with formula (4) with  $\mu = 1$ , and the frequency range  $(\omega_1, \omega_2)$  corresponded with the interval from 1.5 GHz to 2.5 GHz.

**Figure 10**  
Measuring loss tangent. (a) Strip line with an open-circuit stub. (b) Objective function  $\sigma(\text{tg}\delta)|_{\varepsilon'=2.1}$

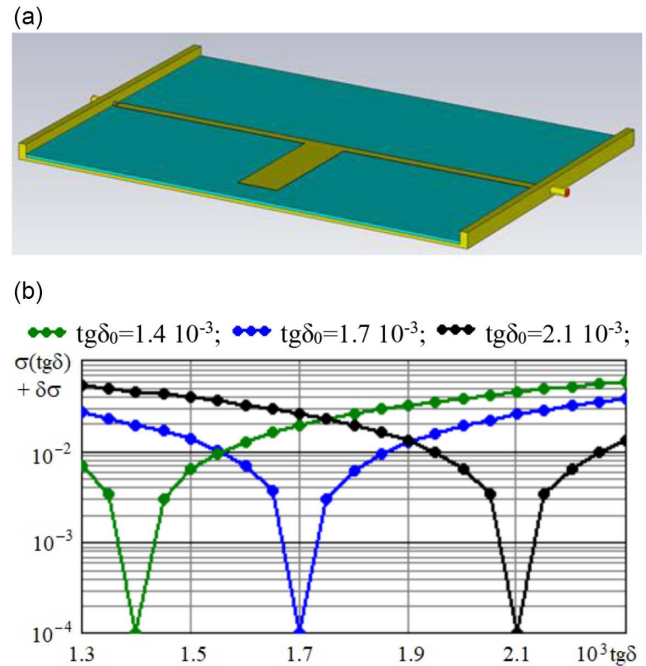


Figure 10a shows the appearance of the fixture with the test plate inserted between the strip and the ground plane. Figure 10b illustrates the behavior of the objective function  $\sigma(\text{tg}\delta)$ , corresponding to function  $\sigma(\varepsilon', g)$  (formula (4) at  $\mu = 1$ ) for each of the mentioned dielectric plates, having equal  $\varepsilon' = 2.1$  and different values of  $\text{tg}\delta_0$  at nominal frequency. For better visualization of the minimization procedure, we use a logarithmic ordinate axis. Therefore, we added the term  $\delta\sigma = 10^{-4}$  to the objective function not only to avoid uncertainty with  $\log(\sigma = 0)$  but also to usefully simulate the contribution of a 1% measurement error in the dependencies  $S_{11}(\omega)$  and  $S_{21}(\omega)$ , which appears in formulas (2)–(4).

To increase the sensitivity of the device and, consequently, the accuracy of measurements of the loss tangent in real conditions, it is necessary to increase the Q factor of the resonator used. This is not a problem. In particular, this can be achieved by lengthening the

resonant stub by a multiple of a quarter wavelength. Not to mention using a system of several stubs or ring resonators.

## 5. Conclusion

This paper presents a strip-line device that serves as a sensor for measuring the complex permittivity of dielectric plates, as well as the corresponding measurement technique. The device is very convenient in practical terms, since it is suitable for testing plates whose thickness, dimensions, and properties of the material vary widely. As for the geometrical constraints, they are very simple: the plate must fit under the strip and within the longitudinal dimension between the ports. This freedom is because the sought parameters (permittivity and loss tangent) are extracted from the measured data, not by formulas, but in the course of computer modeling, which takes into account all the nuances of the plate's geometry and its position.

The simulation results confirm the operability and required sensitivity of the setup. The existence of local minima of the objective function was discovered when measuring the permittivity, and possible ways to overcome this difficulty are discussed.

## Recommendations

If measurements over a sufficiently wide frequency range are required, a universal strip-line device can be developed by connecting in series elements that resonate at different frequencies.

## Acknowledgment

The authors express their gratitude to colleagues from Kazan National Research Technical University, as well as three anonymous reviewers for their kind criticism.

## Ethical Statement

This study does not contain any studies with human or animal subjects performed by any of the authors.

## Conflicts of Interest

The authors declare that they have no conflicts of interest to this work.

## Data Availability Statement

Data are available on request from the corresponding author upon reasonable request.

## Author Contribution Statement

**Yuri Choni:** Conceptualization, Methodology, Formal analysis, Writing – original draft, Writing – review & editing, Visualization. **Vladimir Lavrushev:** Methodology, Software, Formal analysis, Investigation, Visualization. **Alexander Avksentev:** Software, Formal analysis, Writing – review & editing.

## References

- [1] Roberts, S., & Von Hippel, A. (1946). A new method for measuring dielectric constant and loss in the range of centimeter waves. *Journal of Applied Physics*, 17(7), 610–616. <https://doi.org/10.1063/1.1707760>
- [2] Grove, T. T., Masters, M. F., & Miers, R. E. (2005). Determining dielectric constants using a parallel plate capacitor. *American Journal of Physics*, 73(1), 52–56. <https://doi.org/10.1119/1.1794757>
- [3] Parker, G. W. (2002). Electric field outside a parallel plate capacitor. *American Journal of Physics*, 70(5), 502–507. <https://doi.org/10.1119/1.1463738>
- [4] Mitchell, M. R., Link, R. E., & Woolley, D. (2011). Edge correction in calculation of dielectric constant. *Journal of Testing and Evaluation*, 39(2), 1–10. <https://doi.org/10.1520/JTE102715>
- [5] Mamikonyan, B. M., Mamikonyan, Kh. B., Nikoghosyan, D. S., & Abrahamyan, L. S. (2016). Capacitive measuring device. *International Journal of Emerging Engineering Research and Technology*, 4(1), 19–28.
- [6] Agilent Technologies. (2015). *Agilent basics of measuring the dielectric properties of materials*. Massachusetts Institute of Technology. [https://academy.cba.mit.edu/classes/input\\_devices/meas.pdf](https://academy.cba.mit.edu/classes/input_devices/meas.pdf)
- [7] Shkolnik, A. (2015). The measurement and normalisation of dielectric dissipation factor for diagnostics of transformer insulation. *Transformers Magazine*, 2(4), 60–65.
- [8] Chen, L., Ong, C. K., & Tan, B. T. G. (1996). A resonant cavity for high-accuracy measurement of microwave dielectric properties. *Measurement Science and Technology*, 7, 1255–1259.
- [9] Oh, Z. X., Yeap, K. H., Teh, P. C., & Dakulagi, V. (2023). Circular split-ring resonator-based sensor for dielectric constant measurement. *Microwave and Optical Technology Letters*, 65(2), 513–518. <https://doi.org/10.1002/mop.33528>
- [10] Sato, Y., Ogura, N., Yamaguchi, Y., & Ju, Y. (2021). Development of a sensor for dielectric constant measurements utilizing time-domain measurement with a vector network analyzer. *Journal of the International Measurement Confederation*, 169, 108530. <https://doi.org/10.1016/j.measurement.2020.108530>
- [11] Donchenko, A. V., Zargano, G. F., Zemlyakov, V. V., & Kleshchenkov, A. B. (2020). Measurement of the complex permittivity of materials using a double-ridged waveguide. *Journal of Radio Electronics*, 65(5), 427–433.
- [12] Parkhomenko, M. P., Kalenov, D. S., Eremin, I. S., Fedoseev, N. A., Kolesnikova, V. M., & Dyakonova, O. A. (2020). Improving the accuracy of measurements of complex permittivity and magnetic permeability in the microwave range using the waveguide method. *Journal of Radio Electronics*, 65(8), 764–768.
- [13] Maenhout, G., Markovic, T., & Nauwelaers, B. (2021). Controlled measurement setup for ultra-wideband dielectric modeling of muscle tissue in 20–45 °C temperature range. *Sensors*, 21(22), 7644. <https://doi.org/10.3390/s21227644>
- [14] Orend, K., Baer, C., & Musch, T. A. (2022). Compact measurement setup for material characterization in W-band based on dielectric waveguides. *Sensors*, 22(16), 5972. <https://doi.org/10.3390/s22165972>
- [15] Janezic, M. D. (2003). *Nondestructive relative permittivity and loss tangent measurements using a split-cylinder resonator*. Ph.D. Thesis, University of Colorado at Boulder.
- [16] Yashchyshyn, Y., Derzakowski, K., Wu, C., & Cywiński, G. (2021). W-band sensor for complex permittivity measurements of rod shaped samples. *IEEE Access*, 9, 125–131. <https://doi.org/10.1109/ACCESS.2021.3103243>
- [17] Hehenberger, S. P., Caizzzone, S., Thurner, S., & Yarovoy, A. G. (2023). Broadband effective permittivity simulation and measurement techniques for 3-d-printed dielectric crystals. *IEEE*

- Transactions on Microwave Theory and Techniques*, 71(10), 4161–4172. <https://doi.org/10.1109/TMTT.2023.3259479>
- [18] Lee, C. K., Zhang, S., Bukhari, S. S., Cadman, D., Vardaxoglou, J. C., & Whittow, W. G. (2020). Complex permittivity measurement system for solid materials using complementary frequency selective surfaces. *IEEE Access*, 8, 7628–7640. <https://doi.org/10.1109/ACCESS.2020.2963919>
- [19] Sahin, S., Nahar, N. K., & Sertel, K. (2020). Simplified Nicolson-Ross-Weir method for material characterization using single-port measurements. *IEEE Transactions on Terahertz Science and Technology*, 10(4), 404–410. <https://doi.org/10.1109/THZ.2020.2980442>
- [20] Diepolder, A., Mueh, M., Brandl, S., Hinz, P., Waldschmidt, C., & Damm, C. (2024). A novel rotation-based standardless calibration and characterization technique for free-space measurements of dielectric material. *IEEE Journal of Microwaves*, 4(1), 56–68. <https://doi.org/10.1109/JMW.2023.3340448>
- [21] Estévez, J. C., Somolinos, D. R., Gallardo, B. P., & Martínez, D. P. (2023). Development of optimization algorithms for electromagnetic characterization in free space. In *2023 17th European Conference on Antennas and Propagation*, 1–5. <https://doi.org/10.23919/EuCAP57121.2023.10133519>
- [22] Ahmed, A., Kumari, V., & Sheoran, G. (2022). Non-destructive dielectric measurement and mapping using microwave holography. In *2022 2nd Asian Conference on Innovation in Tech. (ASIANCON)*, 1–4. <https://doi.org/10.1109/ASIANCON55314.2022.9909059>
- [23] Krupka, J. (2021). Microwave measurements of electromagnetic properties of materials. *Materials*, 14, 5097. <https://doi.org/10.3390/ma14175097>
- [24] Krylov, V. P., Chirkov, R. A., Zabezhaylov, M. O., & Khramov, A. N. (2024). Solid materials microwave dielectric properties: features of methods practical use. *Izmeritel'naya Tekhnika*, 2, 49–54. <https://doi.org/10.32446/0368-1025it.2024-2-49-54>
- [25] Sonnov, N. V., Leukhin, S. A., & Gerdt, A. D. (2021). Study of dielectric properties of radio-absorbing structural materials. *Microwave Electronics and Microelectronics*, 6(1), 347–350.
- [26] Sheina, E. A., Smirnov, A. P., & Shestopalov, Y. V. (2022). Optimal parameters of a multi-frequency experiment in an inverse problem of determining the dielectric constant of an inclusion in free space and in a waveguide. *Measurements*, 187, 110357. <https://doi.org/10.1016/j.measurement.2022.110357>
- [27] Janezic, M. D., & Krupka, J. (2009). Split-post and split-cylinder resonator techniques: A comparison of complex permittivity measurement of dielectric substrates. *Journal of Microelectronics and Electronic Packaging*, 6, 97–100.
- [28] Alimenti, A., Pittella, E., Torokhtii, K., Pompeo, N., Piuze, E., & Silva, E. (2023). A dielectric loaded resonator for the measurement of the complex permittivity of dielectric substrates. *IEEE Transactions on Instrumentation and Measurement*, 72(2023), 1–9. <https://doi.org/10.1109/TIM.2023.3236301>
- [29] Choni, Y. I., Lavrushev, V. N., & Avksentev, A. A. (2024). *Device for non-destructive measurement of complex permittivity of dielectric plate at microwave frequencies (Russian Patent No. 2822306)*. Federal Institute of Industrial Property. Bulletin 2024/19. Russian.
- [30] Ghattas, A., Al-Sharawi, R., Zakaria, A., & Qaddoumi, N. (2025). Detecting defects in materials using nondestructive microwave testing techniques: A comprehensive review. *Applied Sciences*, 15(6), 3274.
- [31] Liu, W., Ye, M., Yang, F., Yu, G., Zhao, X., & Xie, Y. (2025). Sheet resistance non-destructive test of coated glass using air-gapped microwave cylindrical resonator. *Journal of Nondestructive Evaluation*, 44(2), 45.
- [32] Chaudhary, V. K., Zubair, M., Kazim, J. U. R., Imran, M., & Abbasi, Q. (2025). Performance of Hilbert-curve based microwave sensor for non-destructive testing of CFRP. In *2025 IEEE International Symposium on Antennas & Propagation and North American Radio Science Meeting*.

**How to Cite:** Choni, Y., Lavrushev, V., & Avksentev, A. (2025). Practical Sensor Performance and Methodology for Measuring Permittivity of Dielectric Plates in the Microwave Frequency Range. *Archives of Advanced Engineering Science*. <https://doi.org/10.47852/bonviewAAES52025202>